Production and Trapping of Hydrogenlike and Bare Uranium Ions in an Electron Beam Ion Trap

R. E. Marrs, S. R. Elliott, and D. A. Knapp
Physics Department, Lawrence Livermore National Laboratory, Livermore, California 94550
(Received 10 January 1994)

An equilibrium population of approximately 500 hydrogenlike U^{91+} ions and ten fully stripped U^{92+} ions has been produced and trapped in an electron beam ion trap at 198-keV electron energy. The equilibrium ionization balance, determined from the intensities of radiative recombination x rays, gives values of 1.55 ± 0.27 and 2.82 ± 0.35 b for the electron impact ionization cross sections of hydrogenlike and heliumlike uranium, respectively. These values are somewhat larger than relativistic distorted wave calculations, and much smaller than previous values inferred from stripping of accelerator beams.

PACS numbers: 34.80.Kw, 32.30.Rj

The hydrogenlike isoelectronic sequence of one-electron ions is the simplest atomic system and the only one in which multielectron interactions are completely absent. For this reason the hydrogenlike ions, and atomic hydrogen itself, have been used for many years to obtain fundamental atomic structure information. Experiments include measurements of Lamb shifts, hyperfine splittings, and collision cross sections. The contributions of relativity and QED to atomic energy levels both scale as Z^4, and are therefore most apparent in ions of the highest Z. Hence considerable attention has been given to the measurement of transition energies in hydrogenlike and other few-electron high-Z ions, especially the ions of uranium [1–5]. The electron impact ionization cross sections for the tightly bound $1s$ electrons of high-Z elements are also of interest as a test of relativistic interactions in a simple atomic system. In spite of this interest, even the approximate size of the high-Z ionization cross sections for $1s$ electrons has been uncertain in view of an accelerator stripping measurement that obtained values 3 to 5 times larger than any theory for hydrogenlike and heliumlike uranium [6].

Production of hydrogenlike or bare uranium ions is extremely difficult, requiring many ionizing collisions with small cross sections, at least one of which must have a center-of-mass energy above the 130-keV ionization potential of the uranium $1s$ electrons. These ions have previously been produced only in relativistic (~400 MeV/amu) accelerator beams stripped in foil targets, so x-ray measurements have had to deal with substantial Doppler shift corrections [1–3]. Recently, high velocity U^{91+} and U^{92+} ions have been stored in a ring [4], and deceleration to lower velocities has been proposed. Production of hydrogenlike and bare uranium ions at rest has been a long sought goal.

We report the first production of stationary hydrogenlike and bare uranium ions, along with a measurement of the electron impact ionization cross sections for producing them. The experiments were done with a high energy electron beam ion trap (EBIT) [7] which is an upgrade of an apparatus used previously to obtain the first measurements of electron impact excitation cross sections for very highly charged ions [8]. Approximately 5×10^4 highly charged uranium ions were trapped in the space charge potential of a compressed 198-keV electron beam for times much longer than the roughly 1 sec characteristic time for ionization and recombination of hydrogenlike uranium. We are able to determine the electron impact ionization cross sections of both heliumlike U^{90+} and hydrogenlike U^{91+} from the observed equilibrium ionization balance.

Our high energy EBIT is described in detail elsewhere [7]. A diagram of the trap portion of the apparatus, which operates at a temperature of 4 K, is shown in Fig. 1. The electron beam is compressed and guided along the axis of the trap by a 3-T magnetic field produced by superconducting coils. The electron beam current used in the present work varied from 190 to 205 mA at 198 keV, corresponding to an average current density of 5000 A/cm^2 at a 35-μm beam radius. The compressed beam generates a space charge potential between the axis and beam radius of $V_R = 8.6$ V. The axial trapping voltage, applied by biasing the center and end electrodes, was $V_A = 33$ V, including the change in beam space charge potential due to the different electrode diameters.

Long trapping times require careful control of the ion temperature and energy balance. The trapped ions are continuously heated by Coulomb collisions with beam electrons at a (nonrelativistic) rate given by

$$\frac{dE_i}{dt} = \pi \frac{j_e}{e} \frac{q_i^2 e^4}{E_e} \frac{2m_e}{M_i} \ln\Lambda , \qquad (1)$$

where E_i, q_i, and M_i are the ion energy, charge, and mass, respectively; E_e and j_e are the electron beam energy and current density; e and m_e are the electron charge and mass, and $\ln\Lambda$ is the Coulomb logarithm [9]. For U^{89+} (the most abundant uranium charge state) $dE_i/dt \approx 6$ keV sec^{-1} per ion. Since the radial trapping energy is $q_i V_R \approx 700$ eV, a strong cooling mechanism is clearly required to keep the ions trapped within the beam.

0031-9007/94/72(26)/4082(4)$06.00

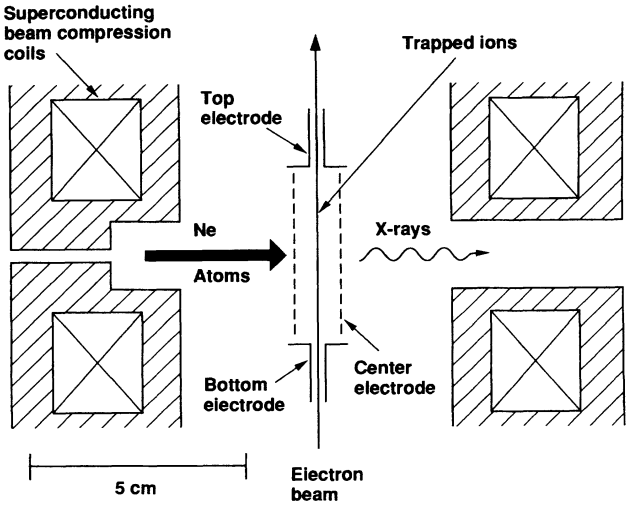

FIG. 1. Trap configuration used in the present experiments. A 35-μm radius, 198-keV electron beam passes along the axis of three electrodes and is compressed by a parallel 3-T magnetic field. The cylindrical center electrode is slotted to facilitate x-ray emission and neon gas injection.

We use an evaporative ion-ion cooling technique to balance the electron beam heating of the uranium ions [10, 11]. A collimated beam of neon atoms with a carefully controlled density crosses the electron beam at 90° as shown in Fig. 1, and roughly 0.2% of the neon atoms that intercept the electron beam are ionized and captured. Electron beam heating of the neon ions is small. They are heated primarily by collisions with uranium ions and reach a high average charge state before escaping axially (evaporating) from the trap with the removal of $q_{\mathrm{Ne}} V_A \approx 300$ eV per neon ion. A detailed computer model of the collision and loss rates in our trap suggests that the uranium ion temperature is about 80 eV, implying that the uranium ions are confined to the center of the electron beam [12].

We use repetitive filling and dumping of our trap to maintain a contaminant-free uranium ion inventory. The trap is initially overfilled by injection of low-charge-state uranium ions from a vacuum spark source [13]. Within roughly 1 sec the uranium inventory and temperature relax to reproducible values determined by the neon cooling rate, with a characteristic time of several minutes for further uranium loss. For the relatively low neutral neon densities used here ($\sim 2 \times 10^5$ cm^{-3} averaged over the length of the trap), the total compensation of the electron beam space charge by neon and uranium charges is less than 10%, and the number of uranium ions in the trap is proportional to (and controlled by) the neutral neon density.

The equilibrium ionization balance for trapped highly charged uranium ions is determined by the relative rates for the ionization and recombination processes that couple adjacent ionization states. The abundance ratio for hydrogenlike and bare uranium at equilibrium is given by

$$\frac{N_{\mathrm{H}}}{N_{\mathrm{bare}}} = \frac{\sigma^{\mathrm{RR}}_{\mathrm{bare}\to\mathrm{H}}}{\sigma^{\mathrm{ion}}_{\mathrm{H}\to\mathrm{bare}}} + \frac{(e/j_e)\, n_0 v \sigma^{\mathrm{CX}}_{\mathrm{bare}\to\mathrm{H}}}{\sigma^{\mathrm{ion}}_{\mathrm{H}\to\mathrm{bare}}}, \qquad (2)$$

where the second term accounts for charge exchange recombination with neutral neon atoms. Here n_0 is the neutral gas density and v is the average ion-neutral collision velocity (approximately the ion thermal velocity). The cross sections for radiative recombination (RR), ionization, and charge exchange (CX) are written in obvious notation. Dielectronic recombination, a resonant process, does not contribute at this energy, and three-body recombination is negligible at EBIT electron energies and densities. Similar equilibrium equations couple other pairs of adjacent charge states. The highest charge states are obtained by keeping the ratio n_0/j_e small. However, since $\sigma^{\mathrm{RR}}_{\mathrm{bare}\to\mathrm{H}}/\sigma^{\mathrm{ion}}_{\mathrm{H}\to\mathrm{bare}} \approx 40$ at our electron energy, it is always true that $N_{\mathrm{bare}} \ll N_{\mathrm{H}}$ and $N_{\mathrm{H}} \ll N_{\mathrm{He}}$. This is in marked contrast to ionization balances at lower Z, where fully stripped ions can be the most abundant species in an EBIT.

We use Eq. (2) and the corresponding expression for $N_{\mathrm{He}}/N_{\mathrm{H}}$ to determine the ionization cross section for the tightly bound $1s$ electrons in both U^{91+} and U^{90+} from the observed values of $N_{\mathrm{H}}/N_{\mathrm{bare}}$ and $N_{\mathrm{He}}/N_{\mathrm{H}}$. We obtain the uranium ionization balance from the RR x-ray spectrum observed at 90° to the electron beam in two cylindrical germanium detectors having active volumes of 40 and 90 cm^3. As can be seen in Fig. 2, the x-ray spectrum consists of a series of peaks corresponding to RR into the open shells of the uranium target ions. X-ray emission from RR into the higher Rydberg levels joins smoothly with bremsstrahlung radiation at the electron beam energy. The electron beam energy spread is known from other measurements [14] to be approximately 100 eV FWHM, so its contribution to the observed peak width is hidden

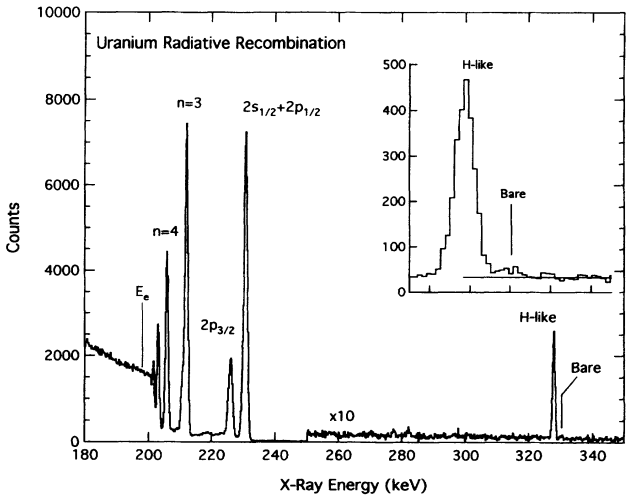

FIG. 2. Radiative recombination spectrum of uranium ions at 198-keV electron energy observed in the 40-cm^3 germanium detector. The inset shows the $n = 1$ feature from the 90-cm^3 detector; the solid horizontal line is the average background level above the peaks.

by the 900-eV FWHM detector resolution. The very weak peaks in the spectrum at approximately 280 and 220 keV are $n = 1$ and $n = 2$ RR of tungsten and osmium contaminants from the cathode of the electron gun.

To confirm that the uranium ionization balance was in equilibrium, x rays were counted for seven 5-sec intervals beginning 7.5 sec after uranium injection. Many injection and counting cycles were added together, and the first time bin was examined for peak ratios different from those in the remaining six time bins; no differences greater than 5% were found. This is consistent with the expected time to reach fully stripped uranium based on assumed values of the cross sections and effective current density. The equilibration time for N_H/N_{bare} is approximately 0.5 sec. The absolute count rate in the different time bins fell by only 8% during the 35-sec counting interval, which means that the uranium loss rate, which is nearly the same for adjacent charge states, was too small to affect the ionization balance. The final summed spectra used to compute the ionization cross sections (displayed in Fig. 2) took 26 h to accumulate.

Having confirmed that the uranium ionization balance is in equilibrium, we obtain the abundance ratios N_H/N_{bare} and N_{He}/N_H from intensity ratios of peaks in the RR spectrum. Radiative recombination cross sections at these electron and x-ray energies are well known from relativistic calculations [15] that agree to within $\sim 3\%$ with extensive measurements of the inverse process of photoionization [16]. The agreement is especially good for photon energies in the range of the present measurement (well above absorption edges); so we adopt $\pm 3\%$ as the uncertainty in the theoretical RR cross sections. For RR into the K shell, $d\sigma^{RR}/d\Omega$ (90°) differs by a factor of 2 for bare and hydrogenlike uranium target ions because the cross section is proportional to the number of K-shell vacancies. (The theoretical ratio is 2.01 due to the small binding energy difference.) Since the $n = 1$ RR lines for bare and hydrogenlike uranium are resolved, a value of $N_H/N_{bare} = 48.5 \pm 7.5$ is directly determined from these lines. The intensity of the weak bare uranium RR line was obtained from a least-squares fit that fixed its width, position, and shape relative to the hydrogenlike RR line, and used a background level determined from the spectral region above the peak. Separate results were obtained from each detector and averaged.

The determination of N_{He}/N_H is more complicated because there is no $n = 1$ RR for heliumlike target ions, and the $n = 2$ RR lines for the different charge states are incompletely resolved. Fortunately, the RR cross section for the open $2s_{1/2}$ orbitals is approximately 5 times larger than for the $2p_{1/2}$ orbitals, so the intensity of the blended $n = 2, j = 1/2$ RR peak is a good indicator of the heliumlike (and lithiumlike) abundance. In contrast, the $n = 3$ RR cross sections are similar for all uranium ions in the trap, so the $n = 3$ RR peak is a good indicator of the total ion inventory. We determine the heliumlike fraction from a fit to the observed ratio of the $n = 2, j = 1/2$ and the $n = 3$ RR peaks with the assumption that the ionization cross section for a $2s$ or $2p$ electron is independent of charge state. We estimate that this procedure contributes a $\pm 5\%$ uncertainty to the heliumlike $1s$ ionization cross section. The hydrogenlike abundance is determined from the $n = 1$ RR line. Radioactive sources were used to measure the energy dependence of the detector efficiencies.

At the neutral neon density used here for observing bare uranium, charge exchange recombination affects the uranium ionization balance. We determined the relative size of the charge exchange term in Eq. (2) from the observed variation in the $RR(2s_{1/2} + 2p_{1/2})/RR(n = 3)$ peak ratio in a series of shorter data runs at neon densities ranging over a factor of 5. To understand the effect of charge exchange, it is helpful to rewrite Eq. (2) as an expression for the ionization cross section:

$$\sigma^{ion}_{H\to bare} = \frac{N_{bare}}{N_H}\left(\sigma^{RR}_{bare\to H} + \langle\sigma^{CX}\rangle\right), \qquad (3)$$

where $\langle\sigma^{CX}\rangle$ is an effective charge exchange recombination cross section given by $\langle\sigma^{CX}\rangle = (e/j_e)\, n_0 v \sigma^{CX}$. The dimensionless quantity $(e/j_e)\, n_0 v$ is much less than one. We find $\langle\sigma^{CX}\rangle = 7.5 \pm 5$ b at the neon density used to determine $\sigma^{ion}_{H\to bare}$ and $\sigma^{ion}_{He\to H}$, compared to total RR cross sections of $\sigma^{RR}_{bare\to H} = 67.5$ b and $\sigma^{RR}_{H\to He} = 43.6$ b [15]. This means that our values for $\sigma^{ion}_{H\to bare}$ and $\sigma^{ion}_{He\to H}$ would be 10% and 15% smaller, respectively, if we did not make the correction for charge exchange. The uranium $1s$ ionization cross sections obtained using Eq. (3) with this correction for charge exchange recombination are given in Table I. The listed uncertainties are quadrature sums of contributions from counting statistics, relative detector efficiency, charge exchange recombination, and (for U^{90+}) the heliumlike fraction.

Assuming independent electrons, it is expected that $\sigma^{ion}_{H\to bare} \approx \frac{1}{2}\sigma^{ion}_{He\to H}$, so our U^{91+} and U^{90+} ionization

TABLE I. Electron impact ionization cross sections for U^{90+} and U^{91+} at 198-keV electron energy in units of 10^{-24} cm^2. The tabulated uncertainties do not include the estimated $\pm 3\%$ uncertainty in the radiative recombination cross sections used for normalization.

Ion	Present experiment	Bevalac[a] experiment	Rel. DW[b] theory	Lotz[c]
$U^{90+}(1s^2)$	2.82 ± 0.35	9.7	1.92	1.5
$U^{91+}(1s)$	1.55 ± 0.27	3.4	0.93	0.7
	(1.41 ± 0.18)[d]	(4.8)[d]		

[a]Values from Ref. [6] multiplied by 0.88 for adjustment to present electron energy (see text). Uncertainties are a factor of 2.
[b]Reference [18].
[c]Reference [17].
[d]$\frac{1}{2}$ of U^{90+} value.

cross sections are really two independent measurements of the same interaction. To emphasize this, we include $\frac{1}{2}\sigma^{\text{ion}}_{\text{He}\to\text{H}}$ in Table I. The only other measurement of the ionization cross sections for hydrogenlike and heliumlike ions of very high-Z elements is an accelerator stripping experiment for uranium at 220-keV equivalent electron energy [6]. These results are compared to our results in Table I after scaling them by $\ln(E_e/I_{1s})/E_eI_{1s}$ to account for the difference in electron energy. (I_{1s} is the $1s$ ionization potential.)

A commonly used semiemperical ionization-cross-section formula due to Lotz [17] has the form

$$\sigma^{\text{ion}}(\text{Lotz}) = 4.5 \times 10^{-14} \sum_j \frac{r_j \ln(E_e/I_j)}{E_e I_j} \quad [\text{cm}^2, \text{eV}], \tag{4}$$

where E_e is the electron energy, I_j is the ionization potential of the jth subshell, and r_j is the number of bound electrons in the jth subshell. Values of σ^{ion}(Lotz) for U^{91+} and U^{90+} are included in Table I, along with the results of a recent relativistic distorted wave calculation [18]. Our measurements suggest that the theoretical cross sections are too low. It is interesting to note that, although the static Coulomb interaction used in the calculations of Ref. [18] is an adequate description of nonrelativistic electron interactions, the transverse (current-current) interaction greatly increases ionization cross sections at relativistic energies. Another calculation of U^{91+} and U^{90+} ionization with relativistic terms in the interaction found significant cancellations at our electron energy and a net effect that is too small to explain our measurement [19].

The ionization balance and the total number of ions in our trap will be important parameters for a variety of future experiments. The total number of uranium ions in the trap can be estimated from the solid angle and efficiency of our x-ray detectors, the known values of $d\sigma^{\text{RR}}/d\Omega\,(90°)$, and an estimate of the effective current density. This gives $N_{\text{total}} \approx 5 \times 10^4$, $N_{\text{H}} \approx 500$, and $N_{\text{bare}} \approx 10$ for our 2-cm long trapping region with the parameters used for the spectrum of Fig. 2. The most abundant ions in the trap are U^{89+} and U^{88+}. At lower Z, N_{bare} can be much larger and we are using the present technique to measure $\sigma^{\text{ion}}_{\text{H}\to\text{bare}}$ for several other elements and electron energies.

In summary, we have produced and trapped both hydrogenlike and bare uranium ions, and measured the electron impact ionization cross section for producing them. The availability of stationary hydrogenlike ions of high-Z elements in an EBIT will facilitate future studies of phenomena such as QED effects, hyperfine splittings, and nuclear-atomic interactions, as well as measurements of other electron-ion collision cross sections and low velocity ion-surface interactions.

We would like to thank J. H. Scofield for calculating the radiative recombination cross sections used for normalization, and K. J. Reed for calculating ionization cross sections. This work was performed under the auspices of the U.S. Department of Energy by Lawrence Livermore National Laboratory under Contract No. W-7405-Eng-48.

[1] C. T. Munger and H. Gould, Phys. Rev. Lett. **57**, 2927 (1986).
[2] J. P. Briand, P. Chevallier, P. Indelicato, K. P. Ziock, and D. D. Dietrich, Phys. Rev. Lett. **65**, 2761 (1990).
[3] J. Schweppe, A. Belkacem, L. Blumenfeld, N. Claytor, B. Feinberg, H. Gould, V. E. Kostroun, L. Levy, S. Misawa, J. R. Mowat, and M. H. Prior, Phys. Rev. Lett. **66**, 1434 (1991).
[4] Th. Stohlker, P. H. Mokler, K. Beckert, F. Bosch, H. Eickhoff, B. Franzke, M. Jung, T. Kandler, O. Klepper, C. Kozhuharov, R. Moshammer, F. Nolden, H. Reich, P. Rymuza, P. Spadtke, and M. Steck, Phys. Rev. Lett. **71**, 2184 (1993).
[5] P. Beiersdorfer, D. Knapp, R. E. Marrs, S. R. Elliott, and M. H. Chen, Phys. Rev. Lett. **71**, 3939 (1993).
[6] N. Claytor, B. Feinberg, H. Gould, C. E. Bemis, J. G. Campo, C. A. Ludemann, and C. R. Vane, Phys. Rev. Lett. **61**, 2081 (1988).
[7] D. A. Knapp, R. E. Marrs, S. R. Elliott, E. W. Magee, and R. Zasadzinski, Nucl. Instrum. Methods Phys. Res., Sect. A **334**, 305 (1993).
[8] R. E. Marrs, M. A. Levine, D. A. Knapp, and J. R. Henderson, Phys. Rev. Lett. **60**, 1715 (1988).
[9] I. P. Shkarofsky, T. W. Johnston, and M. P. Bachynski, *The Particle Kinetics of Plasmas* (Addison-Wesley, Reading, MA, 1966).
[10] M. A. Levine, R. E. Marrs, J. R. Henderson, D. A. Knapp, and M. B. Schneider, Phys. Scr. **T22**, 157 (1988).
[11] M. B. Schneider, M. A. Levine, C. L. Bennett, J. R. Henderson, D. A. Knapp, and R. E. Marrs, in *Proceedings of the International Symposium on Electron Beam Ion Sources and Their Applications*, edited by A. Hershcovitch, AIP Conf. Proc. No. 188 (American Institute of Physics, New York, 1989), p. 158.
[12] B. M. Penetrante, J. N. Bardsley, D. DeWitt, M. Clark, and D. Schneider, Phys. Rev. A **43**, 4861 (1991); B. M. Penetrante (private communication).
[13] I. G. Brown, J. E. Galvin, R. A. MacGill, and R. T. Wright, Appl. Phys. Lett. **49**, 1019 (1986).
[14] D. A. Knapp, P. Beiersdorfer, and D. Schneider (unpublished).
[15] J. H. Scofield, Phys. Rev. A **40**, 3054 (1989); J. H. Scofield (private communication).
[16] E. B. Saloman, J. H. Hubbell, and J. H. Scofield, At. Data Nucl. Data Tables **38**, 1 (1988); A. S. N. Rao, A. Perumallu, and G. K. Rao, Physica (Amsterdam) **124C**, 96 (1984).
[17] W. Lotz, Z. Phys. **216**, 241 (1968).
[18] H. L. Zhang and D. H. Sampson, Phys. Rev. A **42**, 5378 (1990); K. J. Reed (private communication).
[19] M. S. Pindzola, D. L. Moores, and D. C. Griffin, Phys. Rev. A **40**, 4941 (1989).